# A wavelet based drive-by bridge inspection system

# A wavelet based drive-by bridge inspection system

P.J. McGetrick & C.W. Kim
*Dept. of Civil & Earth Resources Eng., Graduate School of Eng., Kyoto University, Kyoto, JAPAN*

ABSTRACT: This paper investigates a low-cost wavelet-based approach for the preliminary monitoring of bridge structures, consisting of the use of a vehicle fitted with accelerometers on its axles. The approach aims to reduce the need for direct instrumentation of the bridge. A time-frequency analysis is carried out in order to identify the existence and location of damage from vehicle accelerations. Firstly, in theoretical simulations, a simplified vehicle-bridge interaction model is used to investigate the effectiveness of the approach. A number of damage indicators are evaluated and compared. A range of parameters such as the bridge span, vehicle speed, damage level and location, signal noise and road roughness are varied in simulations. Secondly, a scaled laboratory experiment is carried out to validate the results of the theoretical analysis and assess the ability of the selected damage indicators to detect changes in the bridge response from vehicle accelerations.

## 1 INTRODUCTION

Research in the field of Bridge Health Monitoring (BHM) over the past two decades has focused on the development and implementation of efficient and effective techniques for bridge structures, such as vibration-based approaches (Carden & Fanning 2004) which require direct instrumentation of bridges with wired or wireless sensors and data acquisition equipment. Such techniques can be effective in highlighting deterioration of bridge condition and are arguably becoming a more critical part of bridge management systems and maintenance strategies, although they can be costly and labour intensive and tend to be aimed towards long span bridges. As large numbers of existing bridges within road networks are not instrumented and are predominantly short to medium span, a more efficient approach is required.

Consequently, there has been a recent focus on the development of indirect vibration-based approaches utilising the response of a vehicle passing over a bridge, a so called 'drive-by' approach. This paper investigates such an approach; an alternative low-cost wavelet-based approach for the monitoring of bridge structures consisting of the use of a vehicle fitted with accelerometers on its axles. The approach aims to detect damage in a bridge while reducing the need for direct instrumentation of the bridge.

The feasibility of using such an indirect approach for bridge condition assessment and the extraction of bridge properties such as frequency, stiffness and changes in damping from the acceleration response of a passing vehicle has been verified theoretically using simulations of vehicle-bridge interaction (VBI) (Yang et al. 2004, Bu et al. 2006, McGetrick et al. 2009, Yang & Chang 2009, González et al. 2012, Keenahan et al. 2012) and its potential for bridge monitoring has also been highlighted in experimental investigations (Lin & Yang 2005, Kim et al. 2011) and field trials (González et al. 2008, Miyamoto & Yabe 2012). An important consideration for the successful implementation of this kind of approach is found to be the dynamic excitation of the bridge; it needs to be sufficiently high to overcome the relatively high influence of road roughness on the vehicle response.

Wavelet theory allows a signal to be analysed in both time and frequency domains simultaneously hence the popularity of its usage in damage identification applications is increasing. Reda Taha et al. (2006) discuss the use of wavelets in health monitoring applications while Nair & Kiremidjian (2009) illustrate the potential of continuous wavelet transforms (CWTs) to be used in statistical pattern recognition approaches for structural damage detection. Their use has also been extended to numerical investigations of indirect approaches which aim to identify localised damage within a bridge from the wavelet transform of vehicle displacements (Nguyen & Tran 2010, Khorram et al. 2012) and accelerations (McGetrick & Kim 2013); low speeds are found to be beneficial and the approach can be more effective than using fixed sensors on the bridge.

In order to investigate the effectiveness of the wavelet-based drive-by system in detecting damage in a bridge, this paper extends the analysis carried out by McGetrick & Kim (2013) to other test conditions and compares alternative damage indicators, utilising VBI models in theoretical simulations and a laboratory experiment.

## 2 MODELLING & SCENARIOS

### 2.1 *Theoretical vehicle-bridge interaction model*

A coupled VBI model described by McGetrick et al. (2013) is used in theoretical simulations (Fig. 1). It consists of a 4 degree of freedom half-car model crossing over a finite element (FE) beam at constant speed; they are coupled at their points of contact. The body and axle masses of the vehicle are $m_s$ = 16200 kg, $m_{u,1}$ = 700 kg and $m_{u,2}$ = 1100 kg respectively. The suspension and tire spring linear stiffness coefficients for axle 1 are $K_{s,1} = 4 \times 10^5$ N/m and $K_{t,1} = 1.75 \times 10^6$ N/m respectively while the corresponding values for axle 2 are $K_{s,2} = 1 \times 10^6$ N/m and $K_{t,2} = 3.5 \times 10^6$ N/m respectively. The suspension viscous damping coefficients are $C_{s,1} = 10 \times 10^3$ Ns/m and $C_{s,2} = 20 \times 10^3$ Ns/m. The sprung mass moment of inertia, $I_s$, is 93234 kgm$^2$. The distances of the axles to the centre of gravity, $o$, are $D_1$=2.85 m and $D_2$=1.9 m. Finally, the vehicle's frequencies of vibration are $f_{v,1}$ = 1.1 Hz, $f_{v,2}$ = 1.4 Hz, $f_{v,3}$ = 8.8 Hz and $f_{v,4}$ = 10.2 Hz corresponding to body bounce, body pitch and the hop of axles 1 and 2 respectively. The properties of the bridge spans used in simulations are given in Table 1; each span has 3% damping. The coupled system is solved using the Wilson-theta integration scheme (Tedesco et al. 1999). A sampling frequency of 100 Hz is used in simulations. To damage the beam, percentage stiffness reductions are applied to individual elements, representing localised damage within the bridge. Acceleration measurements, $\ddot{y}_{s,i}$, are recorded above the axles as shown in Figure 1.

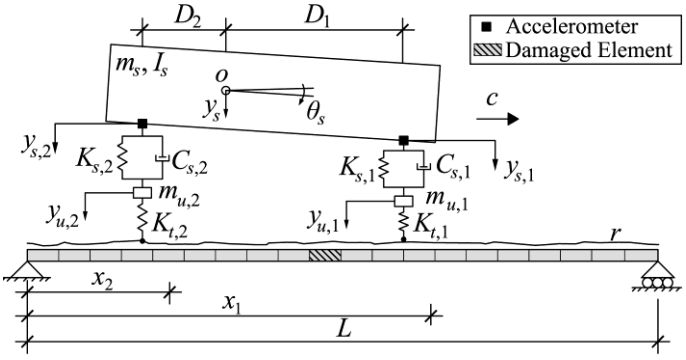

Figure 1.Vehicle-bridge interaction model.

Table 1 Finite element beam properties

| Span Length (m) | Intact Element Stiffness (N m$^2$) | Mass per unit length (kg/m) | 1st natural frequency of vibration, $f_{b,1}$ (Hz) |
|---|---|---|---|
| 15 | $1.846 \times 10^{10}$ | 28 125 | 5.66 |
| 25 | $4.865 \times 10^{10}$ | 18 358 | 4.09 |
| 35 | $1.196 \times 10^{11}$ | 21 752 | 3.01 |

### 2.2 *Experimental model*

Figure 2 shows the experimental setup which included a scaled two–axle vehicle with axle spacing of 0.4 m, fitted with 2 accelerometers at axle centres to monitor bounce motion. A wireless router and data logger allowed accelerations to be recorded remotely. A constant vehicle speed was maintained by an electronic controller and each bridge crossing was repeated 5 times. Three speeds were adopted; S1 = 0.93 m/s, S2 = 1.16 m/s and S3 = 1.63 m/s. Two vehicles were used, V1 and V2, of masses 21.6 kg and 25.8 kg respectively. Their bounce frequencies were both 2.93 Hz while pitch frequencies were 3.9 Hz and 3.7 Hz respectively. The scaled bridge model was a simply supported steel beam of span 5.4 m which incorporated a scaled road surface profile. It had frequency $f_{b,exp}$ = 2.6 Hz, mass per unit length of 52 kg/m and stiffness of 120,700 N m$^2$. It was fitted with accelerometers at mid-span and quarter points to measure its response during vehicle crossings. For the experiment, damage was applied via 0.7 m long rectangular saw-cuts in the beam's flanges between midspan and 3/8ths of the span. Four scenarios were investigated: Intact, D1, D2 and D3 corresponding to no damage, 5 mm, 10 mm and 15 mm cuts respectively (Fig. 2(c)). A sampling frequency of 100 Hz was used in the experiment.

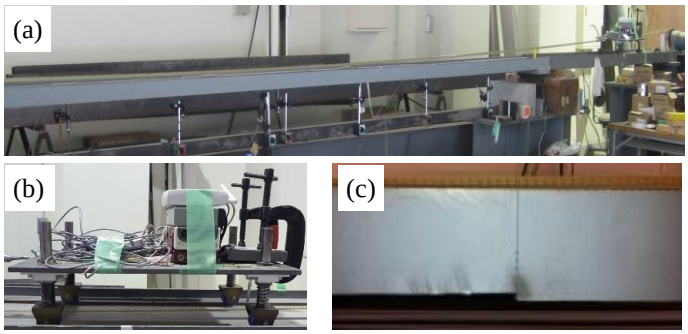

Figure 2. Experiment setup (a) Beam (b) Vehicle (c) Saw cut

### 2.3 *Continuous Morlet wavelet transform and pattern adapted wavelet basis*

The continuous wavelet transform (Mallat 2008) of a function $f(t) \in L^2(\mathbf{R})$ is given as

$$Wf(a,b) = \int_{-\infty}^{\infty} f(t) \frac{1}{\sqrt{a}} \psi^* \left( \frac{t-b}{a} \right) dt \qquad (1)$$

where * indicates the complex conjugate of the mother wavelet function, $\psi(t) \in L^2(\mathbf{R})$, which has zero-mean and is scaled by *a* and translated by *b*, given by Equation 2,

$$\psi_{a,b}(t) = \frac{1}{\sqrt{a}}\psi\left(\frac{t-b}{a}\right) \tag{2}$$

The mother wavelet adopted for this investigation is the real valued symmetrical Morlet wavelet, as used by McGetrick & Kim (2013) and described by Equation 3,

$$\psi(t) = e^{-\frac{t^2}{2}}\cos(5t) \tag{3}$$

Time localisation is an important criterion in order to detect damage location and the Morlet wavelet provides an appropriate balance between time and frequency resolution for this purpose. Therefore the Morlet CWT of vehicle acceleration responses is adopted as a damage sensitive feature.

In addition to the Morlet wavelet basis, a pattern-adapted wavelet basis (Mesa 2005) is formulated for comparison. This is based on a damage pattern extracted from the vehicle acceleration signal due to an arbitrary bridge stiffness change. The following steps are completed in order to formulate a basis for this study:

1 Record representative healthy and damaged acceleration signal samples and calculate the difference between them
2 Select a portion of the signal difference corresponding to damage and fit a pattern to it which is admissible as a wavelet
3 Store this new basis in a directory from which it can be called by CWT functions within Matlab

The length of the selected portion is chosen in order to provide an appropriate balance between time and frequency resolution. The new pattern-adapted wavelet basis is defined on the interval [0, 1].

#### 2.3.1 *Damage indicator*

The CWTs of the differences between healthy and damaged accelerations obtained in theoretical simulations and the experiment are analysed in both time and frequency domains simultaneously for the purpose of damage detection. All source acceleration signals are normalized using their standard deviations before calculating the differences and applying the CWT. Peaks occurring in the wavelet coefficients indicate the existence and location of damage. A damage indicator based on the maximum magnitude of these peaks at particular frequencies is established and compared for both Morlet and pattern-adapted wavelet bases. It focuses on frequencies related to the vehicle as they are the most dominant in the VBI.

## 3 RESULTS DISCUSSION

### 3.1 *Theoretical simulations*

In simulations, the aim is to investigate the effectiveness of the wavelet-based approach in identifying the existence and location of damage in a bridge for a range of parameters. Bridge span lengths of 15 m, 25 m and 35 m, vehicle speeds of 2 m/s, 5 m/s, 10 m/s and 20 m/s, vehicle masses of 9 tonnes and 18 tonnes, a perfectly smooth profile and a total number of 51 rough road profiles are tested. The effect of contaminating acceleration measurements with additive white Gaussian noise of signal-to-noise ratio (SNR) of 20 is investigated. The damage level and location are also varied; stiffness reductions from 1% up to 20% are applied to an individual beam element at 3*L*/8, *L*/2 or 5*L*/8.

Results are presented in this section for simulations using the Morlet wavelet basis, unless otherwise stated, and for measurements above axle 2 only; similar results were found for those above axle 1. A comparison between damage indicators from both Morlet and pattern-adapted wavelet bases is included.

#### 3.1.1 *Effect of bridge span length*

In Figure 3, solid parallel vertical lines indicate the entry/exit of the axle time of the axle on the damaged beam element while the crossing dashed lines mark the time and frequency of the maximum wavelet coefficient. Hence, it can be seen that for all span lengths, 1% damage at midspan is located in the wavelet coefficients at peaks which correspond to the vehicle frequency of 1.4 Hz. Also, as the bridge span length increases, the peak coefficient magnitudes increase and the resolution in time improves due to the longer time history of VBI available for analysis. However, peaks at the bridge frequency occurring at other times become more significant; indicating that the approach may be more effective for locating damage in longer spans provided the vehicle and bridge frequencies do not coincide.

#### 3.1.2 *Effects of vehicle speed and mass*

Figures 4(a) and (b) highlight that as speed increases to 5 m/s and 20 m/s respectively for the 18 t vehicle, the time and frequency resolutions and maximum magnitude decrease considerably due to the shorter VBI time. However, the damage can still be detected and appears to be located more accurately for 20 m/s, despite the bridge and vehicle frequency peaks merging.

By inspecting Figure 4(c), it can be seen that reducing the vehicle mass to 9 t provides a slight improvement in damage localisation compared to Figure 3(a) for the 18 t vehicle, although the maximum coefficient does not vary significantly. This improvement is most likely due to the increase in vehicle frequency caused by the decrease in mass. How-

ever, the response at the bridge frequency also increases across the spectrum which may have a negative impact on locating damage for longer spans.

3.1.3 *Effects of damage location and level*

Figure 5 illustrates the effect of varying the damage location and level. Comparing with Figure 3(a), it can be observed in Figures 5(a) and (b) that 1% damage is detected and located in elements at 3*L*/8 and 5*L*/8 with similar accuracy and peak magnitude.

The effect of increasing the damage level at midspan to 10% is illustrated by Figure 5(c). The only significant effect observed is the increase of coefficient magnitudes proportional to the increase in damage, which suggests that magnitudes may potentially be used to quantify damage.

3.1.4 *Effects of signal noise and road roughness*

Contaminating acceleration measurements with noise of signal-to-noise ratio (SNR) of 20, it is found that above a damage severity of approximately 1%, the damage can still be located at the coefficient peak at the vehicle frequency. Figure 6(a) shows the corresponding results for 5% damage at midspan. Here, the contaminated acceleration signals are low pass filtered below 8 Hz before being processed by the CWT as the main frequencies of interest are less than this. Due to the added noise, the peak becomes slightly more difficult to distinguish.

Results presented thus far have been for ideal conditions with a perfectly smooth road profile. In reality, the road surface will not be perfectly smooth. Hence, a range of 51 randomly generated 'very good' class A road profiles (ISO 1995) were tested in simulations with no noise.

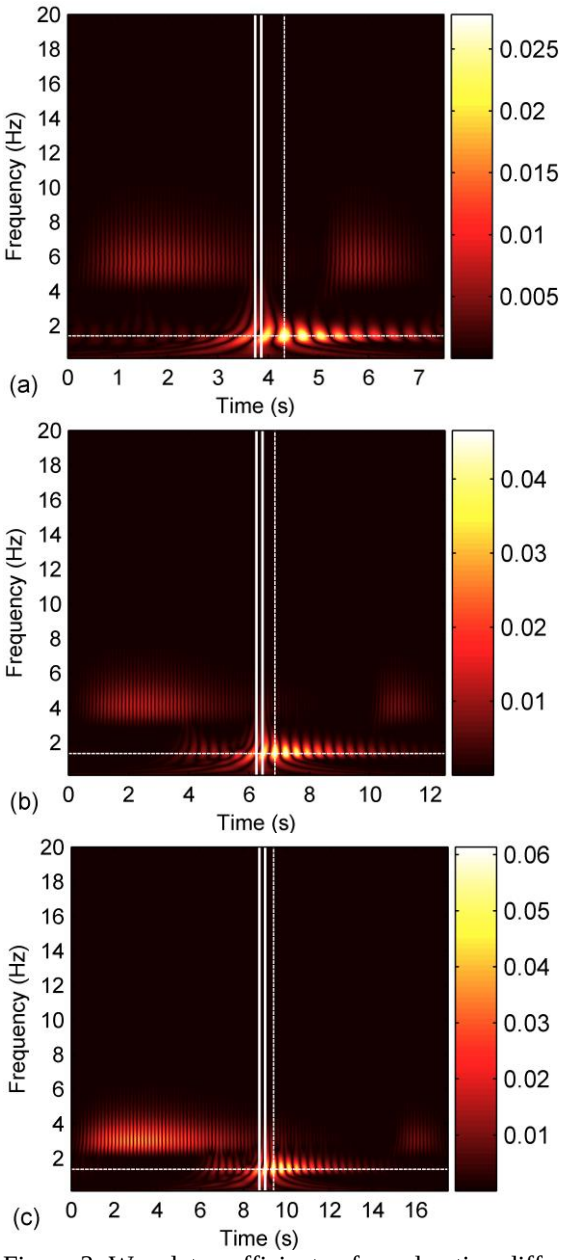


Figure 3. Wavelet coefficients of acceleration difference above axle 2 on (a) 15 m span (b) 25 m span (c) 35 m span; speed is 2 m/s, 18t vehicle, 1% damage at *L*/2, smooth road profile.

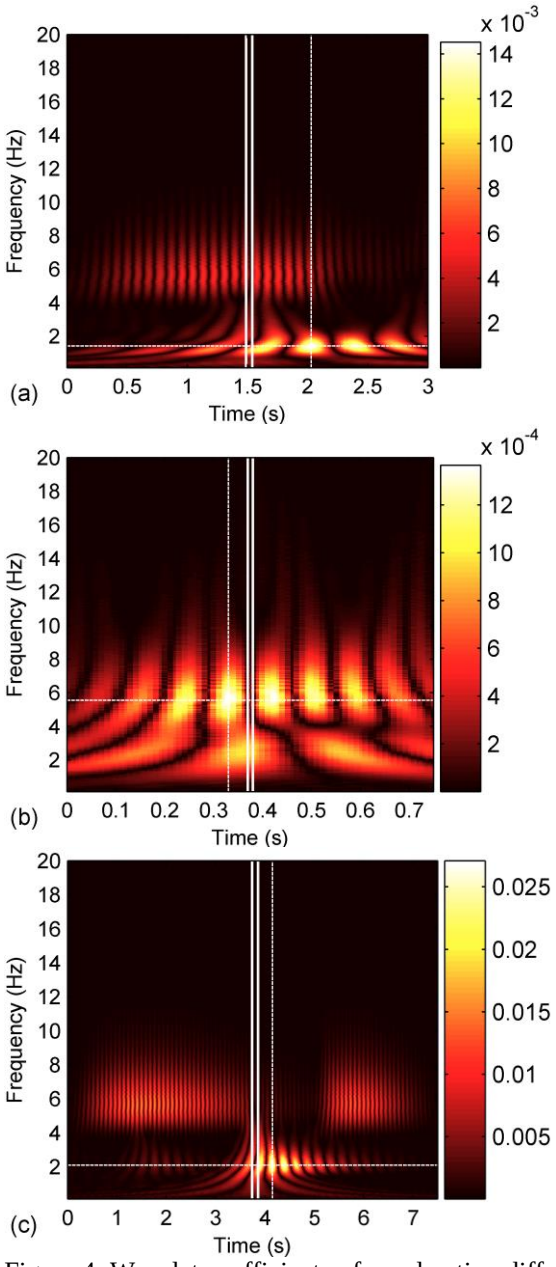


Figure 4. Wavelet coefficients of acceleration difference above axle 2 for 15 m span (a) 18t at 5 m/s (b) 18t at 20 m/s (c) 9t at 2 m/s; 1% damage at *L*/2, smooth road profile.

It is found that the damage can be detected in the vehicle response, as for the smooth profile. This can be seen in the example given in Figure 6(b), although the magnitudes of the coefficients are much lower for the rough road profile compared to Figure 3(a).

### 3.1.5 *Comparison of damage indicators from Morlet and pattern-adapted wavelets*

To illustrate the effectiveness of the approach overall for all 51 rough profiles tested, a damage indicator (DI) based on the maximum coefficient on the frequency range $[f_{v,2}/2, (f_{v,2}+f_{b,1})/2]$ is calculated and plotted in Figure 7(a) for all speeds and profiles tested for the 15 m span and Morlet wavelet basis. To allow comparison between the DIs for all damage levels, they are standardised for each speed using their means and standard deviations.

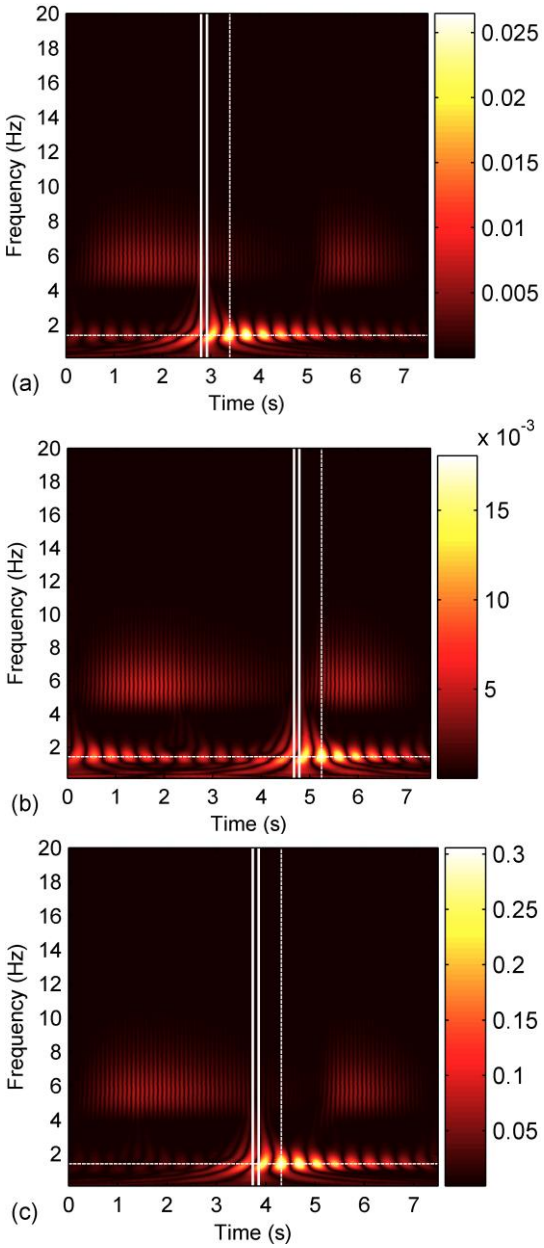


Figure 5. Wavelet coefficients of acceleration difference above axle 2 (a) 1% damage at 3*L*/8 (b) 1% damage at 5*L*/8 (c) 10% damage at *L*/2; speed is 2 m/s, 18t vehicle, 15 m span, smooth road profile.

DIs for all speeds are grouped in Figure 7(a) according to the damage level. It is clear from this figure that damage can be detected and also, as the damage increases, so too does the selected DI. This highlights that the DI could be effective for both damage detection and quantification while it is not significantly affected by speed.

Figure 7(b) summarizes the results for identifying damage location; damage level was found to have no effect hence only one level is shown here. The mean errors as percentages of the bridge span length are 11.9%, 17.3%, 4.4% and 20.6% for 2, 5, 10 and 20 m/s respectively. The identified location does not vary significantly with road profile. Here, the accuracy appears to be the best for 10 m/s which may be due to higher excitation of the bridge, or an error due to resolution.

Figure 8 illustrates the results for a pattern-adapted wavelet basis for the purposes of comparison with Figure 7. The basis has been formulated using the steps given in Section 2.3 utilising vehicle accelerations from a simulation of one of the 51 profiles, tailored for the measurements above axle 2. It should be noted by inspecting Figure 8(a) that the selected pattern is actually more sensitive to the damage location at the bridge frequency therefore a more appropriate DI, corresponding to the maximum coefficient at this frequency, is chosen.

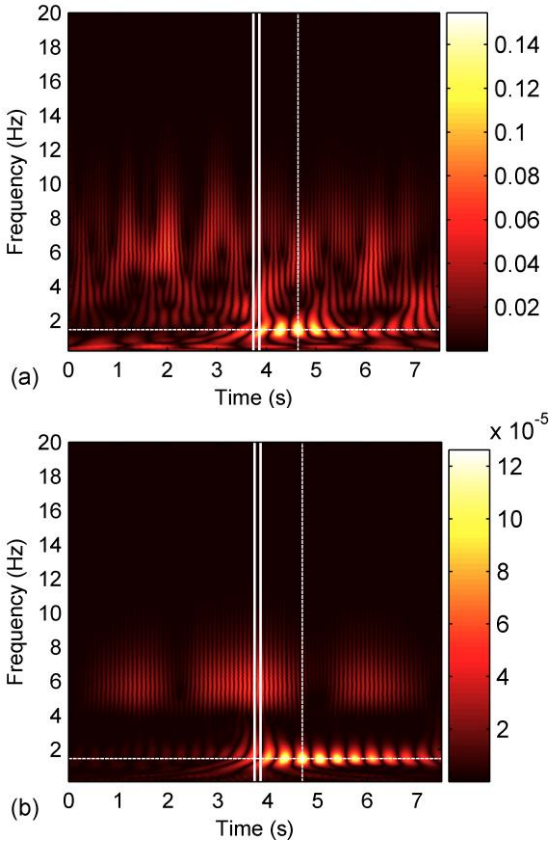


Figure 6. Wavelet coefficients of acceleration difference above axle 2 for 18t vehicle on 15m span with damage at *L*/2 (a) smooth profile with SNR = 20 and 5% damage (b) very good profile and 1% damage; speed is 2 m/s.

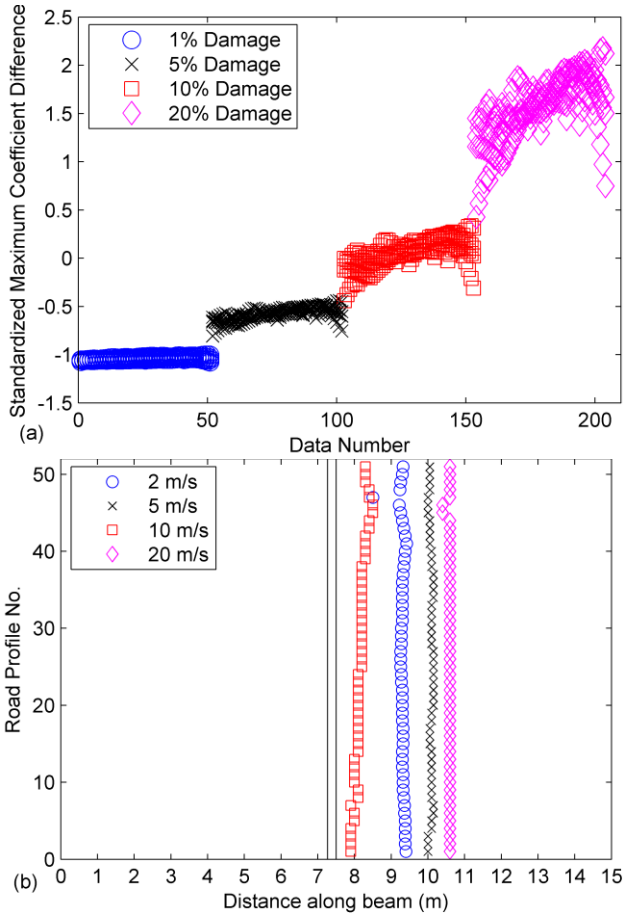


Figure 7. Morlet wavelet basis results (a) identified DIs (b) identified damage locations; 18t vehicle, 15m span with damage at *L*/2, 51 ISO class A profiles

It is found that this DI, shown in Figure 8(b), follows a similar pattern to that in Figure 7(a), although it provides slightly more overlap between damage levels. However, despite this, the mean percentage errors in location (Fig. 8(c)) have decreased to 3.9%, 5.5%, 6.4% and 10.2% for 2, 5, 10 and 20 m/s respectively. This indicates that while using the pattern-adapted wavelet basis could make it slightly more difficult to quantify damage compared to the Morlet wavelet; it increases the identified damage location accuracy.

## 3.2 *Laboratory Experiment*

The results of the experiment are summarized here for axle 2 of the vehicle, which was found to be more accurate due to its frequency. Figure 9(a) shows an example of the wavelet coefficients obtained for the acceleration difference between Intact and D3 scenarios for vehicle V1 using the Morlet wavelet; the largest peaks occur at the start of the time history at the vehicle frequency of 3.7 Hz before the vehicle reaches the damage location, indicating that global rather than local changes are significant due to this damage. Figure 9(b) shows the equivalent results for the scenario in Figure 9(a) for a pattern-adapted wavelet basis, adapted to the pattern along the damaged section for axle 2 acceleration differences between the Intact and D1 scenarios.

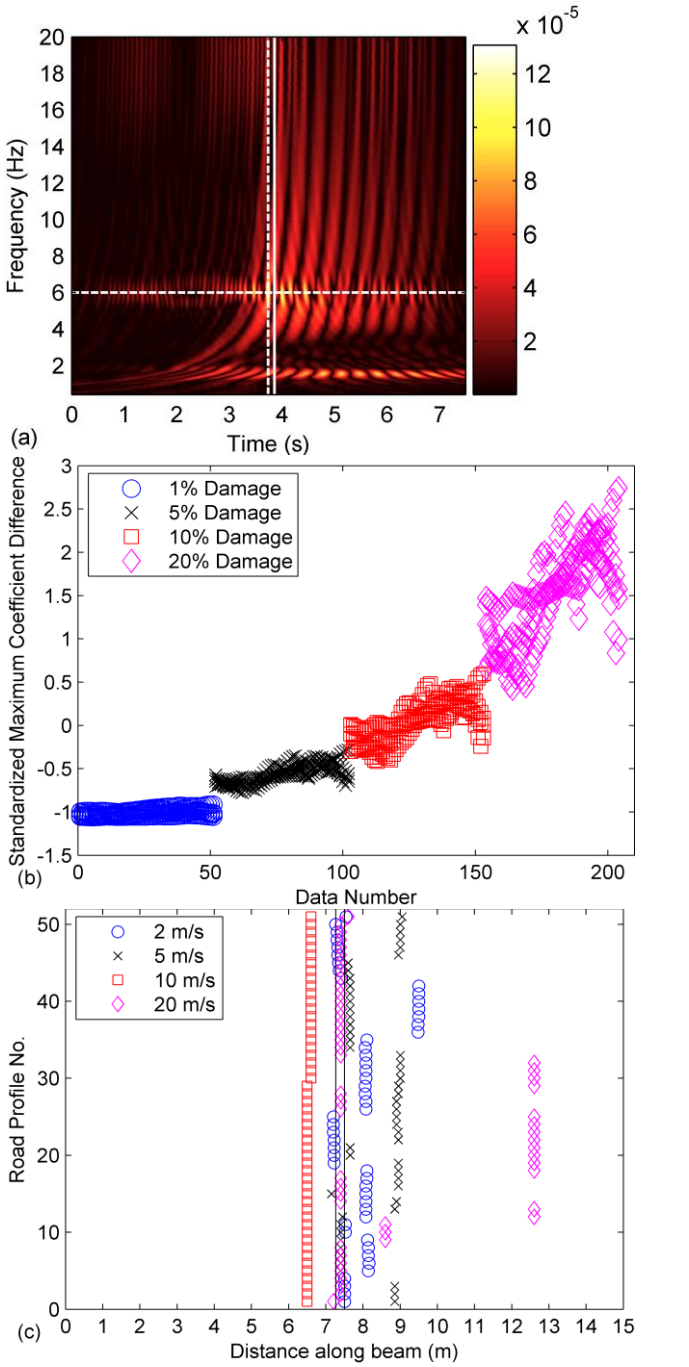


Figure 8. Pattern-adapted wavelet basis results (a) Example of wavelet coefficients of acceleration difference above axle 2 (b) identified DIs (c) identified damage locations; 18t vehicle, 15m span with damage at *L*/2, 51 ISO class A profiles

Results are similar to those for the Morlet wavelet although the pattern-adapted wavelet's maximum coefficient is closer to the damaged location. In addition to the global effect of the damage, differences between the damage pattern for D1 and D3 may cause this inaccuracy.

### 3.2.1 *Experimental damage indicators*

Figure 10(a) shows the experimental damage indicators calculated for all speeds, tests and damage scenarios for vehicle V1 using the Morlet wavelet basis. It is clear that the indicator is not as sensitive here as in simulations; D2 is difficult to distinguish from D1. However, D3 can be distinguished from D1 more easily. Speed is not found to have a significant

effect. Figure 10(b) shows the corresponding results for the pattern-adapted wavelet basis which show a similar trend. Similar results are also observed for vehicle V2, omitted here. These results suggest that a pattern-adapted wavelet basis could be used to improve the identification of damage location without significantly affecting the DI or its trend with increasing damage.

## 4 CONCLUSIONS

This paper investigates a wavelet-based drive-by system for the monitoring of bridge structures which consists of the use of a vehicle instrumented with accelerometers on its axles. In theoretical simulations, it is found that the approach can detect and locate bridge damage more accurately for lower vehicle speeds and longer bridge spans due to time resolution. The damage is detected at the vehicle frequency response for smooth and rough road profiles but it is more difficult to locate in the presence of signal noise unless the damage level exceeds 1%.

A damage indicator based on wavelet coefficients of the difference between healthy and damaged accelerations allows different levels of damage to be detected and distinguished from each other. Indicators are formed and compared for the Morlet wavelet basis and a pattern-adapted wavelet basis and it is found that the latter is more sensitive to the damage location while the former is more suitable for quantifying the damage level.

In a laboratory experiment damage can be detected but it is found to be more difficult to distinguish between damage scenarios using the damage indicators. Experimental results also highlight that the pattern-adapted wavelet basis is more sensitive to the damage location.

Overall, this investigation has illustrated the potential of this low-cost approach and highlighted conditions within which it can detect and/or locate bridge damage with reasonable accuracy. Further work is required to address challenges associated with the real-world application of this approach.

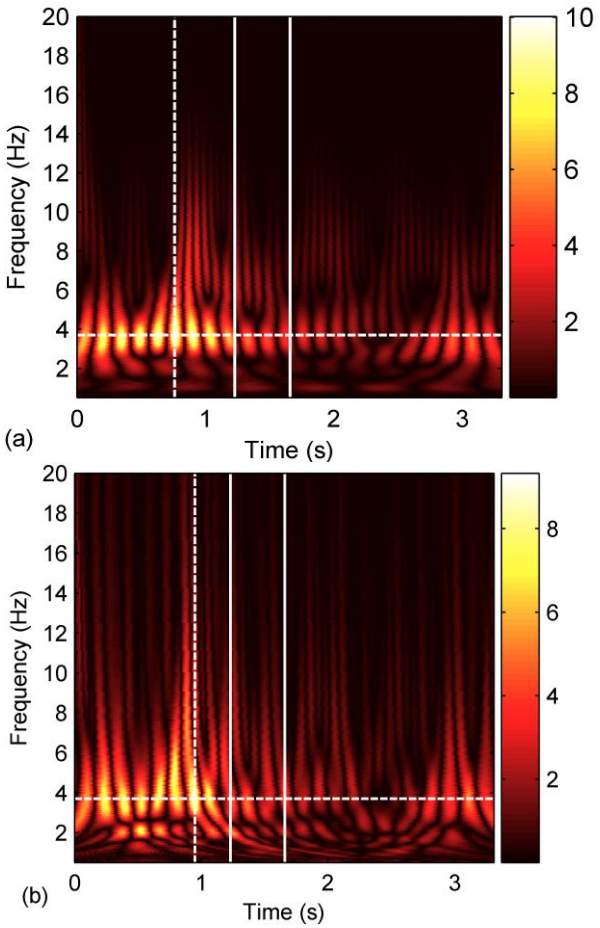


Figure 9. Wavelet coefficients of acceleration difference above axle 2 for vehicle V1 and speed S3 in experiment (a) Morlet wavelet coefficients (b) Pattern-adapted wavelet coefficients

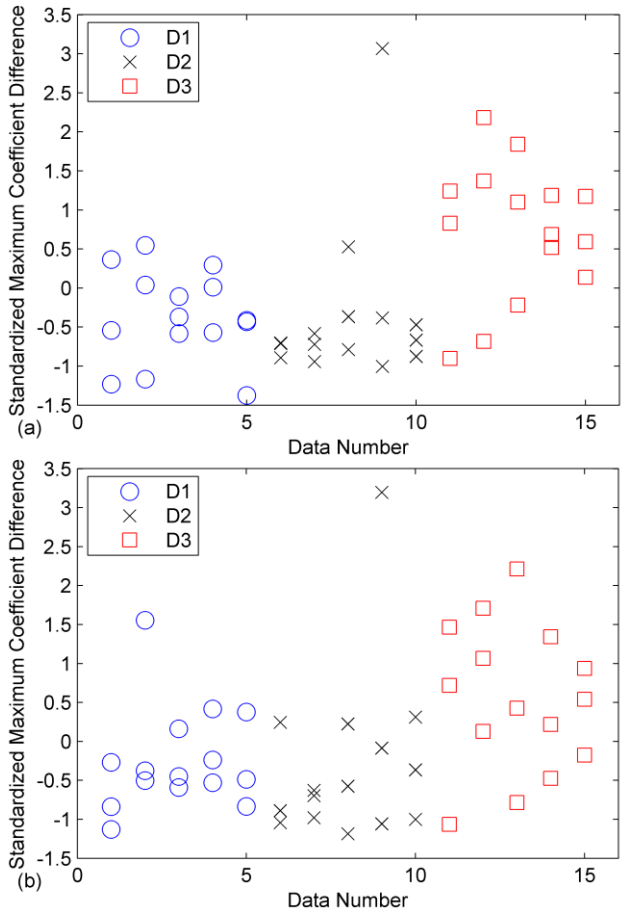


Figure 10. Identified DIs from experiment for vehicle V1 and all speeds and tests using (a) Morlet wavelet (b) Pattern-adapted wavelet

## 5 ACKNOWLEDGEMENTS

The authors wish to express their gratitude for the financial support received from the Japanese Society for the Promotion of Science for the Grant-in-Aid for Scientific Research (B) under project no. 24360178.

## 6 REFERENCES

Bu, J.Q., Law, S.S. & Zhu, X.Q. 2006. Innovative bridge condition assessment from dynamic response of a passing vehicle. *Journal of Engineering Mechanics, ASCE* 132(12): 1372-1379.

Carden, E.P. & Fanning, P. 2004. Vibration based condition monitoring: A review. Structural Health Monitoring, 3(4): 355-377.

González, A., Covián, E. & Madera, J. 2008. Determination of Bridge Natural Frequencies Using a Moving Vehicle Instrumented with Accelerometers and GPS. *Proceedings of the Ninth International Conference on Computational Structures Technology, Athens, Greece*, Paper 281.

González, A., OBrien, E.J. & McGetrick, P.J. 2012. Identification of damping in a bridge using a moving instrumented vehicle. *Journal of Sound and Vibration* 331(18): 4115-4131.

ISO 8608. 1995. *Mechanical Vibration-road Surface Profiles-reporting of Measured Data*. International Standards Organisation.

Keenahan, J., McGetrick, P.J., OBrien, E.J. & González, A. 2012. Using Instrumented Vehicles to Detect Damage in Bridges, *Proceedings of the 15th International Conference on Experimental Mechanics, Porto, Portugal*, Paper 2934.

Khorram, A., Bakhtiari-Nejad, F. & Rezaeian, M. 2012. Comparison studies between two wavelet based crack detection methods of a beam subjected to a moving load. *International Journal of Engineering Science* 51: 204-215.

Kim, CW, Isemoto, R, Toshinami, T, Kawatani, M, McGetrick, PJ, & OBrien, E.J. 2011. Experimental investigation of drive-by bridge inspection. *5th International Conference on Structural Health Monitoring of Intelligent Infrastructure (SHMII-5), Dec. 11-15*, Cancun, Mexico.

Lin, C.W. & Yang, Y.B. 2005. Use of a passing vehicle to scan the fundamental bridge frequencies. An experimental verification. *Engineering Structures* 27: 1865-1878.

Mallat, S. 2008. *A Wavelet Tour of Signal Processing, Third Edition: The Sparse Way*. Academic Press.

McGetrick, P.J., González, A. & OBrien, EJ. 2009. Theoretical investigation of the use of a moving vehicle to identify bridge dynamic parameters. *Insight* 51(8): 433-438.

McGetrick, P.J., Kim, C.W., González, A. & OBrien, E.J. 2013. Dynamic Axle Force and Road Profile Identification using a Moving Vehicle. *International Journal of Architecture, Engineering and Construction* 2(1): 1-16.

McGetrick, P.J. & Kim, C.W. 2013. A parametric study of a drive by bridge inspection system based on the morlet wavelet. *Key Engineering Materials* 569-570: 262-269.

Mesa, H. 2005. Adapted Wavelets for Pattern Detection. In SANFELIU, A. & CORTÉS, M. (eds), *Progress in Pattern Recognition, Image Analysis and Applications*. Springer Berlin Heidelberg.

Miyamoto, A. & Yabe, A. 2012. Development of practical health monitoring system for short- and medium-span bridges based on vibration responses of city bus. *Journal of Civil Structural Health Monitoring* 2: 47-63.

Nair, K.K. & Kiremidjian, A.S. 2009. Derivation of a Damage Sensitive Feature Using the Haar Wavelet Transform. *Journal of Applied Mechanics, ASME* 76(6): 1-9.

Nguyen, K.V. & Tran, H.T. 2010. Multi-cracks detection of a beam-like structure based on the on-vehicle vibration signal and wavelet analysis. *Journal of Sound and Vibration* 329(21): 4455-4465.

Reda Taha, M.M., Noureldin, A., Lucero, J.L. & Baca, T.J. 2006. Wavelet transform for structural health monitoring: a compendium of uses and features. *Structural Health Monitoring* 5(3): 267-295.

Tedesco, J.W., McDougal, W.G. & Ross, C.A. 1999. *Structural Dynamics, Theory and Applications*. Addison-Wesley, Boston, United States.

Yang, Y.B., Lin, C.W. & Yau, J.D. 2004. Extracting bridge frequencies from the dynamic response of a passing vehicle. *Journal of Sound and Vibration* 272: 471-493.

Yang, Y.B. & Chang, K.C. 2009. Extracting the bridge frequencies indirectly from a passing vehicle: Parametric study. *Engineering Structures* 31(10): 2448-2459.